

Research Article

Prescribed-Time Fractional Order Control of DWR via Time-Varying Scaling Function

Pengfei Zhang ^{1,2}, Qiyuan Chen ^{1,3} and Ye Chen ^{1,2}

¹School of Engineering, Huzhou University, Huzhou, Zhejiang, China

²Huzhou Key Laboratory of Intelligent Sensing and Optimal Control for Industrial Systems, School of Engineering, Huzhou University, Huzhou 313000, China

³Hangzhou Zhongce Vocational School Qiantang, Hangzhou, Zhejiang, China

Correspondence should be addressed to Ye Chen; cy0004@163.com

Received 19 June 2023; Revised 5 September 2023; Accepted 22 September 2023; Published 9 October 2023

Academic Editor: A Kushari

Copyright © 2023 Pengfei Zhang et al. This is an open access article distributed under the Creative Commons Attribution License, which permits unrestricted use, distribution, and reproduction in any medium, provided the original work is properly cited.

This study focuses on a differential wheeled robot's (DWR) prescribed-time fractional order position control. Firstly, based on the kinematic model of DWR, a distance-related orientation error is designed using the inverse sine function. Based on this, an improved linear velocity constraint function is proposed. Compared with existing methods, while ensuring the correlation between velocity and orientation error, the multibalance point risk caused by large angle errors is avoided. Then, a prescribed-time fractional order position controller based on a time-varying scaling function is proposed to stabilize the kinematic system of DWR in the prescribed time. This controller can stabilize the position control system of the DWR in a prescribed time by adjusting the prescribed-time parameter, avoiding the infinite gain risk in traditional prescribed-time controllers. Finally, through numerical simulation, we verify that the proposed control law can converge the system status of DWR to the bounded interval in the prescribed time.

1. Introduction

Due to their simple structure and strong stability, differential wheel robots (DWR) have been widely used in intelligent logistics and medical rescue scenes, bringing many conveniences to people's daily lives [1–3]. For example, the DWR is a mobile base equipped with a flexible robotic arm to complete the pick-up task [4–6]. In some practical applications, especially material-handling scenarios, mobile robots often must reach the target location within the specified time [7]. In these applications, the robot can reduce the distance from the target position by controlling its linear and angular velocities. This motivation, also known as “position stabilization,” has received widespread attention from researchers.

The literature contains a variety of approaches to this topic. In the literature [5, 6], the author studies the maximum load of the manipulator when the flexible manipulator is installed on the mobile robot. The finite element method can be applied to derive kinematic and dynamic equations for moving carriers [5]. Furthermore, reference [6] proposed

a new method for path planning for a wheeled mobile manipulator using hierarchical optimal control. Based on the robot kinematic model, the authors of literature [8] use PID control to provide a reference speed for the robot-driving wheel. Literatures [9, 10] have the experiments of the control law in [8]. Compared to the previous works, the linear velocities in [9, 10] consider the orientation error, which ensures that the speed is slow when the robot's orientation does not meet expectations. Complex technologies are proposed in other studies, such as adaptive [11] or predicting controllers [12], but the settling time of the robot position control system is not precise. However, in practical applications, such as material-handling scenarios, robots need to complete tasks within a limited time [13]. Although the angle error is considered in the velocity design of DWR [9, 10], thereby reducing the nonlinear coupling relationship of the system, it still cannot obtain an accurate association between the stability time and speed. More importantly, if the system's settling time can be accurately obtained, it can improve the work efficiency of the robot to a certain extent

[5]. Conventional finite-time control makes the system stable within a finite time affected by initial values, which is not conducive to practical applications [14]. Fixed-time control provides a prespecifiable upper bound for the system settling time, independent of the initial state value but still influenced by design parameters [15]. In [16, 17], the authors propose a new finite-time control method based on a time-varying scaling function with a monotonous increasing characteristic called prescribed-time control (PTC). The characteristic of PTC is that the system's settling time can be predetermined within the allowed physical range, independent of the initial state values and system parameters. However, the controller gain of PTC will gradually increase to infinity with the running time, which cannot ensure the system's continuity after the prescribed time. For this reason, literature [18] introduced a time-varying piecewise function. It proposed an adaptive PTC method for robot systems, but the method did not consider the application of higher-order systems. In [19], a prescribed-time robust differentiator was designed based on an event-triggered approach using finite varying gains. Further, literature [20] introduced a switching scaling function to obtain a prescribed finite time state feedback controller for higher-order systems. Also, in literature [21], a new notion of stability, called triangular stability, is proposed, and triangular stability implies prescribed-time stability. The piecewise time-varying function avoids the infinite gain problem faced at time T by switching in advance, making the system state known after the prescribed time [18–21]. However, due to the sampling time of the DWR control system, when the switching delay is triggered, the problem of reverse gain may occur, causing the system to diverge. Therefore, the PTC method suitable for the DWR position control system is still worth further studies.

This paper is developed from the above literature and is aimed at designing the prescribed-time position controller suitable for the DWR control system. The main work is as follows:

- (1) The novel orientation error and linear velocity constraint functions are provided based on the DWR kinematic model. Compared with [9], the method in this paper not only keeps the yaw angle of the DWR at the target point at zero but also solves the problem of misalignment of the balance point caused by excessive orientation error
- (2) A time-varying scaling function suitable for the DWR position control is proposed by introducing a fractional power term. When applying this scaling function to the prescribed-time position control of DWR, not only does it avoid the problem of infinite gain, but also the stability time of the DWR position control system can be predetermined by adjusting the time parameter

The rest of this paper is arranged as follows. Section 2 provides the relevant variables for the position control system of the DWR. The prescribed-time fractional order position controller designed in this paper is given in Section 3,

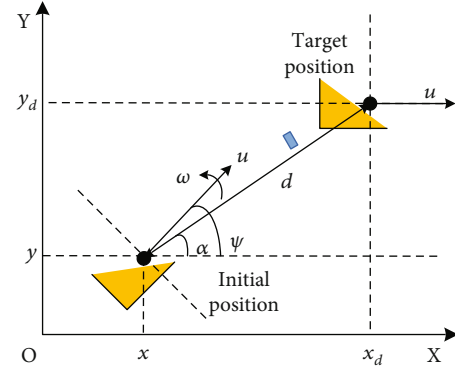


FIGURE 1: Basic model of DWR.

and the stability of the proposed controller is analyzed in Section 4. Numerical simulations and discussions are presented in Section 5.

2. System Modeling and the Objective

This section proposes an innovative orientation error, and then, we point out that the position control problem of DWR can be described as the stabilization control of its kinematic model.

Differential wheeled robots (DWR) rely on two drive wheels perpendicular to the wheel axis for movement. The DWR changes the driving direction by the speed difference between the two drive wheels, so it does not need additional steering movement to complete the turning. Figure 1 shows the primary variables of DWR in the position control movement. We used the DWR kinematic model from literature [9] that does not consider the sway.

$$\begin{cases} \dot{x} = u \cos \psi, \\ \dot{y} = u \sin \psi, \\ \dot{\psi} = \omega. \end{cases} \quad (1)$$

The states x , y , and ψ are the centroid positions and the yaw angle of the robot in the coordinate system, respectively. The u and ω represent the linear and angular velocities of the robot, respectively, and are used as the system's input.

The initial position is (x, y) , and the target position is (x_d, y_d) . Then, the distance between the two is d , and the azimuth angle is defined as α .

$$d = \sqrt{(x_d - x)^2 + (y_d - y)^2}, \quad (2)$$

$$\alpha = a \tan 2(y_d - y, x_d - x). \quad (3)$$

Now, taking the time derivative of (2) and replacing (1), we can obtain

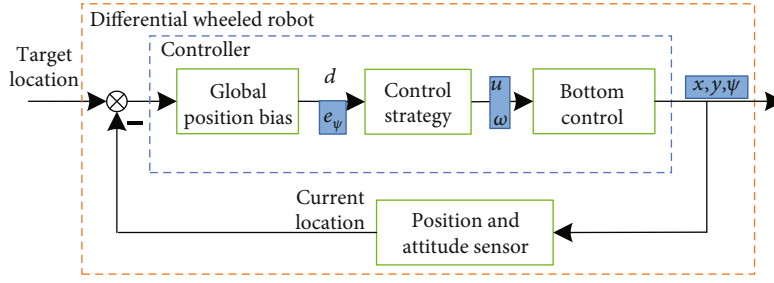


FIGURE 2: Basic process of position control.

$$\begin{aligned} \dot{d} &= -\frac{\dot{x}(x_d - x) + \dot{y}(y_d - y)}{d} = -u(\cos \alpha \cos \psi + \sin \alpha \sin \psi) \\ &= -u \cos(\alpha - \psi). \end{aligned} \quad (4)$$

From (3),

$$\dot{\alpha} = \frac{(y_d - y)\dot{x} - (x_d - x)\dot{y}}{d^2} = \frac{u \sin(\alpha - \psi)}{d}. \quad (5)$$

Then, we propose an innovative orientation error

$$e_\psi = \alpha - \psi + \zeta, \quad \zeta = \sin^{-1}[k\alpha \tanh(d)], \quad (6)$$

where $0 \leq k \leq 1/(2\pi)$, and auxiliary arcsine function ζ satisfies $-\pi/6 \leq \zeta \leq \pi/6$. Moreover, the interval of $\alpha - \psi$ has been given in [9], which satisfies $(\alpha - \psi) \in [-\pi, \pi]$. Then, e_ψ satisfies $-7\pi/6 \leq e_\psi \leq 7\pi/6$. From (4),

$$\begin{aligned} \dot{e}_\psi &= \dot{\alpha} - \dot{\psi} + \dot{\zeta} = \frac{u \sin(e_\psi - \zeta)}{d} \\ &\quad - \omega + k \frac{\dot{\alpha} \tanh(d) + \alpha [1 - \tanh^2(d)] \dot{d}}{\sqrt{1 - [k\alpha \tanh(d)]^2}}. \end{aligned} \quad (7)$$

The following transformed kinematic system is obtained:

$$\begin{cases} \dot{d} = -u \cos(e_\psi - \zeta), \\ \dot{e}_\psi = \frac{u \sin(e_\psi - \zeta)}{d} - \omega + k \frac{\dot{\alpha} \tanh(d) + \alpha [1 - \tanh^2(d)] \dot{d}}{\sqrt{1 - [k\alpha \tanh(d)]^2}}. \end{cases} \quad (8)$$

Therefore, if $d \rightarrow 0$ can be achieved while u and ω remain bounded, the position control of the robot is completed. Further, this paper is aimed at designing the corresponding prescribed-time velocity control law for u and ω so that the robot can start from any initial position and achieve $d \rightarrow 0$ in a predetermined time T_{con} . Moreover, the prescribed-time T_{con} is an arbitrary preadjustable parameter. In short, the control objective can be described as the following formula $\lim_{t \rightarrow T_{\text{con}}} (d, e_\psi) = 0$.

Figure 2 shows the basic process of the robot position control. The robot relies on the sensor to obtain the distance and angle information, and the controller relies on these two values to get the linear and angular velocities. Subsequently, the execution agency controlled the wheels to rotate according to the speed instruction to complete the movement.

Remark 1. It is noteworthy that when $k=0$, $e_\psi = \alpha - \psi$, which becomes the case of the study in [9]. In [9], the controller adjusts the robot's yaw angle by driving $\alpha - \psi \rightarrow 0$ (i.e., $e_\psi \rightarrow 0$). However, this method makes the robot's yaw angle at the endpoint uncontrollable. With regard to function ((6)) proposed in this paper, we have $\dot{\alpha} \rightarrow -u \sin \zeta/d = -uk\alpha \tan h(d)/d$ when $e_\psi \rightarrow 0$. Therefore, by designing the u to drive $\alpha \rightarrow 0$ and $\psi \rightarrow 0$, we can ensure that the yaw angle of the DWR remains $\psi = 0$ when the target position is reached.

In theory, this transformation has ambiguity at the origin. There are two main reasons for using this method in this paper:

- (1) This method is applicable to practical engineering and has practicality. This is because after using the Euler system, the positioning control can become a linear system, making it easy to adjust convergence properties. Therefore, many recent excellent achievements in DWR positioning control are also using this method, such as [9]
- (2) In engineering, we can theoretically avoid singularity by switching the control to lead out the origin, such as controlling the speed to 0 when the distance is less than 1 cm or less. Therefore, this method has good application value in engineering

3. Prescribed-Time Fractional Order Position Controller Design

Firstly, a novel constraint function is proposed based on existing orientation errors to optimize the correlation between the robot linear velocity and angle. Subsequently, a novel time-varying scale function is proposed based on the conventional PTC method, and the DWR's prescribed-time fractional order control laws are formulated.

3.1. System Transformation and Objective. When the DWR is far from the target position and the orientation error is

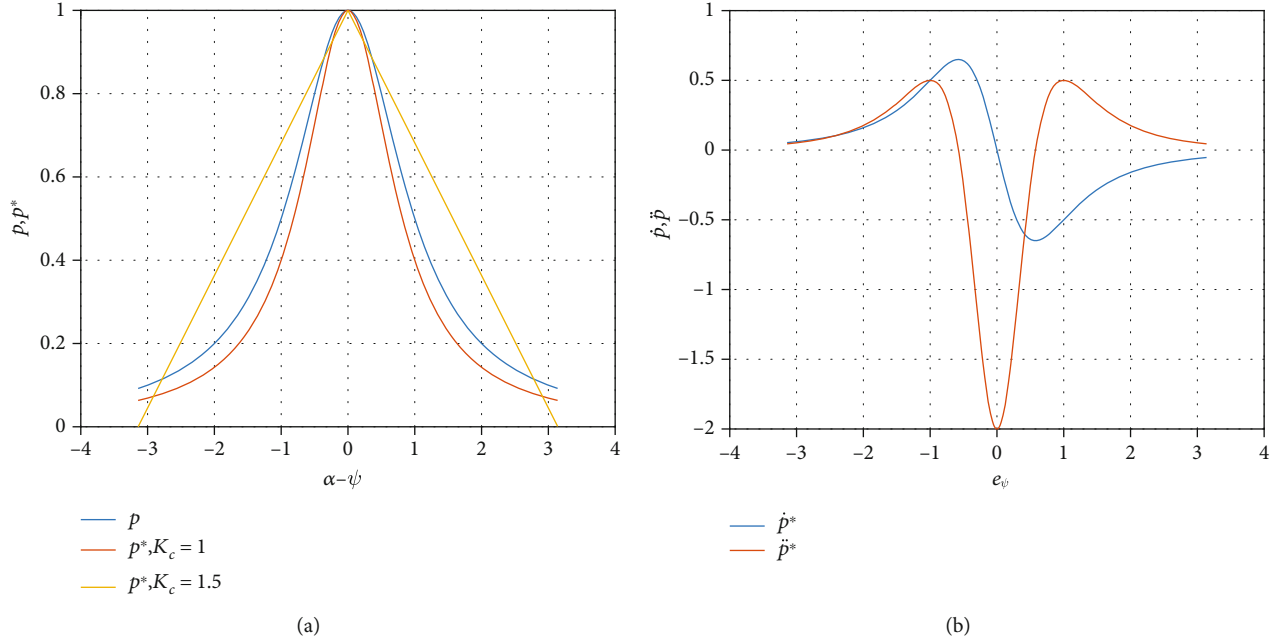


FIGURE 3: p vs. p^* . (a) First-order partial derivative image. (b) Numerical graph of $\dot{p}^*(e_\psi)$ and $\ddot{p}^*(e_\psi)$.

large, it is more desirable for the robot to reach the correct orientation first. The current work [9] links the linear velocity with angular error and provides a control law for the linear velocity as follows:

$$u = K_0 dp, p = \frac{\pi - |\alpha - \psi|}{\pi}, \quad (9)$$

where $K_0 > 0$ is an optional parameter and the constraint function p satisfies $0 \leq p \leq 1$. The linear velocity is a nonlinear function related to the angular error $|\alpha - \psi|$. The use of the constraint auxiliary function p makes it possible for the linear velocity to be dismissed depending on the angular error $|\alpha - \psi|$.

For the previous control law (9), when the angular error $(\alpha - \psi) = \pm\pi$, there is $p = 0$. The previous constraint auxiliary function p gives the linear velocity control law (6) that can be adjusted for the angular error $(\alpha - \psi)$, but it has an unwanted behavior for the value of $(\alpha - \psi) = \pm\pi$ (see Figure 3). In this region, the DWR's line velocity command will incorrectly output zero. As a result of this behavior, the DWR's control system is at risk of misalignment of the balance point. To avoid the above, we have improved p to obtain a novel linear velocity constraint function

$$p^* = \frac{1}{1 + K_e(\alpha - \psi + \zeta)^2} = \frac{1}{1 + K_e e_\psi^2}, \quad (10)$$

which satisfies $0 < p^*(e_\psi) \leq 1$; $K_e > 0$ is an optional parameter. Notice that due to (6), the interval of values of e_ψ is restricted to $e_\psi \in [-(7/6)\pi, (7/6)\pi]$.

Consider constraint functions $p(z) = p = (\pi - |z|)/\pi$ and $p^*(z) = 1/(1 + K_e z^2)$, where $z \in \mathcal{R}$ is the composite state vector. The partial derivatives of $p(z)$ and $p^*(z)$ are given:

$$\frac{\partial p(z)}{\partial z} = \begin{cases} -\frac{1}{\pi}, z > 0 \\ 0, z = 0 \\ \frac{1}{\pi}, z < 0 \end{cases}, \quad \frac{\partial p^*(z)}{\partial z} = \frac{-2K_e z}{(1 + K_e z^2)^2}. \quad (11)$$

Obviously, the partial derivative of $p(z)$ is discontinuous at $z = 0$, while $p^*(z)$ has the characteristic of a continuous partial derivative. Therefore, using p^* to replace p in the existing velocity control law can make the control action of the controller smoother.

Remark 2. Compared with [9], the new constraint function (10) satisfies $p^* > 0$. When applied to the controller of DWR, the linear velocity is kept at zero only when the distance is zero, which can avoid the risk of misaligned control system balance points. Moreover, function (14) can slowly increase the linear velocity of the robot when the angle error is significant. Then, function (10) has better smoothness, which allows the robot's trajectory to be further optimized.

3.2. Prescribed-Time Fractional Order Position Controller. First, we briefly introduce the basic principles of the prescribed-time control (PTC). The key in the PTC is the utilization of the time-varying scaling function (12) with monotonically increasing characteristics [16].

$$\mu_1(t, T) = \frac{T}{T + t_0 - t}, \quad (12)$$

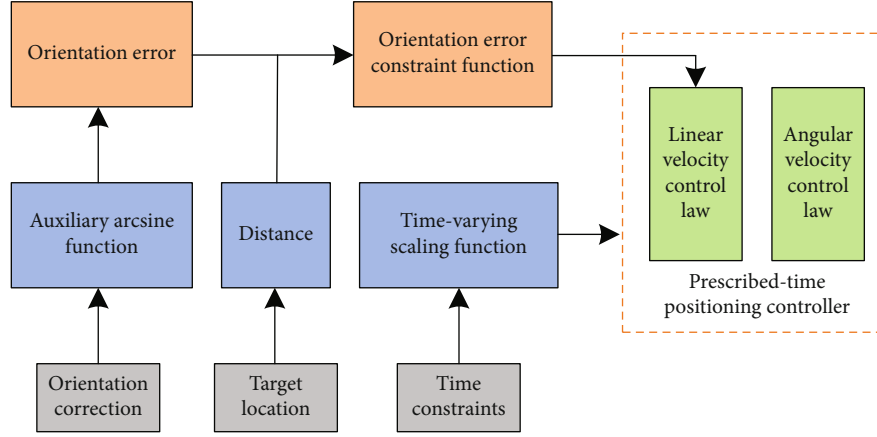


FIGURE 4: Controller structure.

where $T > 0$ with the properties that $\mu_1(t_0, T) = 1$ and $\mu_1(t_0 + T, T) = +\infty$. The function (12) starts at $t = t_0$ and has increased to infinity as $t \rightarrow t_0 + T$.

Lemma 3 (see [16]). Consider the function

$$\mu(t, T) = \frac{T^{n+m}}{(T + t_0 - t)^{n+m}} = \mu_1(t, T)^{n+m}, \quad T > 0, \quad (13)$$

on $t \in [t_0, t_0 + T)$, with positive integers n and m . t_0 denotes the initial time, and n corresponds to the order of the system. A continuous function $V : [t_0, t_0 + T) \rightarrow (0, +\infty)$ satisfies

$$\dot{V}(t) \leq -2\kappa\mu(t, T)V(t) + \frac{\mu(t, T)}{4\lambda}\xi(t)^2, \quad (14)$$

for positive constants κ and λ , where $\xi(t)$ is a disturbance. Then, solving the above differential inequality can obtain

$$V(t) \leq \exp \left\{ -\frac{2\kappa T}{n+m-1} [\mu_1(t-t_0)^{n+m-1} - 1] \right\} V(t_0) + \frac{\|\xi\|_{[t_0, t]}^2}{8\kappa\lambda}, \quad \forall t \in [t_0, t_0 + T). \quad (15)$$

Corollary 4. Consider Lemma 3; if $\xi(t) \equiv 0$, then $\lim_{t \rightarrow t_0 + T} V(t) = 0$. That is, in the absence of disturbance $\xi(t)$, the differentiable function $V(t)$ is prescribed-time stable in T .

Corollary 4 is one case of Lemma 3. Its function will be demonstrated in the following text to demonstrate the stability and settling time of the system. According to Lemma 3, the effective time of conventional PTC is only applicable to the time $t \in [t_0, t_0 + T)$. When $t \rightarrow t_0 + T$, the controller gain gradually increased to an infinitely large value, and the system status of the system was unknown after T . Subsequently, combined with the constrained auxiliary function (10) proposed in the previous section, the linear velocity control law is designed as follows:

$$u = K_1 \mu^*(t, T_{\text{con}}) p^* d^{2\beta-1}. \quad (16)$$

And a novel time-varying scaling function is given as

$$\mu^*(t, T_{\text{con}}) = \begin{cases} \frac{1}{T_{\text{con}} - t}, & 0 \leq t \leq t_v \\ \frac{1}{T_{\text{con}} - t_v}, & t > t_v \end{cases}, \quad (17)$$

$$t_v = T_{\text{con}} \left\{ 1 - \exp \left[\frac{-(d_0^2 + e_{\psi 0}^2)^{1-\beta}}{(1-\beta)2Kp_{\min}^*} \right] \right\},$$

where the fractional order parameter β satisfies $1/2 < \beta < 1$. K_1, K are adjustable parameters, satisfying $K_1, K > 0$ and $t_v \leq T_{\text{con}}$. $T_{\text{con}} > 0$ is a prescribed-time parameter that can be customized by the user. In addition, d_0 denotes the initial value of the distance, $e_{\psi 0}$ denotes the initial value of the directional error, and p_{\min}^* is the minimum value of p^* .

Besides, in order to stabilize the DWR control system, the angular velocity control law was obtained based on the backstepping method.

$$\omega = du\Delta + \dot{\alpha} + k \frac{\dot{\alpha} \tanh(d) + \alpha [1 - \tanh^2(d)] \dot{d}}{\sqrt{1 - [k\alpha \tanh(d)]^2}} + K_2 p^* \mu^*(t, T_{\text{con}}) |e_{\psi}|^{2\beta-1} \text{sign}(e_{\psi}), \quad (18)$$

$$\Delta = \frac{1 - \cos(e_{\psi} - \zeta)}{e_{\psi} - \zeta}, \quad (19)$$

where $K_2 > 0$, $K \leq \min\{0.6K_1, K_2\}$, and $\lim_{e_{\psi} - \zeta \rightarrow 0} ((1 - \cos(e_{\psi} - \zeta))/(e_{\psi} - \zeta)) = 0$. $1 - \cos(e_{\psi} - \zeta)$ is the high-order infinitesimal of $e_{\psi} - \zeta$. The basic idea of the controller is shown in Figure 4.

Remark 5. In the actual navigation process of the DWR, the distance d and orientation error e_ψ can be obtained through simple measurement of the sensor. Therefore, the initial distance d_0 and the initial azimuth $e_{\psi 0}$ are considered to be known a priori. Compared with [16, 17], the novel time-varying scaling function (17) effectively avoids the singularity problem of the traditional PTC and extends the effective time of the scaling function to $t \in [t_0, t_0 + T_{\text{con}})$.

Generally speaking, the two-wheel speed of DWR does not require a state estimator to estimate the position but can be directly obtained through an encoder or Hall sensor. From this, the forward speed and angular velocity in the current state can be directly obtained. The acquisition of position and angle information can also be directly achieved by sensors without the need for further research. In engineering, if the acquisition of these quantities is unstable, some filtering methods can be used for estimation. However, these estimation algorithms are generally built-in to the sensor or independent of the control methods studied in this paper and can be directly integrated with the methods in this paper. Therefore, this paper will not study this issue here.

4. Stability Analysis and Parameter Choosing

In this section, the stability of the proposed controller is analyzed, and recommendations for the selection of adjustable parameters are given.

4.1. Stability Analysis. Before proceeding with the stability analysis, we first introduce the following lemma.

Lemma 6 (see [22]). *Let $x, y > 0$ and $\gamma > 0$. Then,*

$$\begin{aligned} x^\gamma + y^\gamma &\geq (x + y)^\gamma, & 0 < \gamma \leq 1, \\ x^\gamma + y^\gamma &\geq 2^{1-\gamma}(x + y)^\gamma, & \gamma > 1. \end{aligned} \quad (20)$$

We use this lemma to simplify the proof process of the control system stability. Second, we give the following theorem.

Theorem 7. *The kinematic system (8) is stable for a prescribed time under the action of the control laws (16) and (18). Moreover, the convergence time of the system (8) can be determined by the prescribed-time parameter T_{con} .*

Proof. Choose the following Lyapunov function

$$L = \frac{1}{2} \left(d^2 + e_\psi^2 \right). \quad (21)$$

Now, taking the time derivative of (21), we get

$$\begin{aligned} \dot{L}(t) &= -du \cos(e_\psi - \zeta) + e_\psi \left[\dot{\alpha} - \omega + \frac{k(\dot{d}\alpha + d\dot{\alpha})}{d_{\text{max}} \sqrt{1 - (kd\alpha/d_{\text{max}})^2}} \right] \\ &= -du + du[1 - \cos(e_\psi - \zeta)] \\ &\quad + e_\psi \left[\dot{\alpha} - \omega + \frac{k(\dot{d}\alpha + d\dot{\alpha})}{d_{\text{max}} \sqrt{1 - (kd\alpha/d_{\text{max}})^2}} \right]. \end{aligned} \quad (22)$$

Substituting the auxiliary function Δ , and $-0.4 \leq \Delta\zeta \leq 0.4$, we can obtain

$$\begin{aligned} \dot{L}(t) &= -du(1 + \Delta\zeta) + e_\psi \left[du\Delta + \dot{\alpha} - \omega + \frac{k(\dot{d}\alpha + d\dot{\alpha})}{d_{\text{max}} \sqrt{1 - (kd\alpha/d_{\text{max}})^2}} \right] \\ &\leq -0.6du + e_\psi \left[du\Delta + \dot{\alpha} - \omega + \frac{k(\dot{d}\alpha + d\dot{\alpha})}{d_{\text{max}} \sqrt{1 - (kd\alpha/d_{\text{max}})^2}} \right]. \end{aligned} \quad (23)$$

We substitute the proposed control laws (16) and (18) into the above equation to obtain

$$\dot{L}(t) \leq -\mu^*(t, T_{\text{con}}) p^* \left(0.6K_1 d^{2\beta} + K_2 e_\psi^{2\beta} \right). \quad (24)$$

We have defined the minimum value of p^* as p_{min}^* ,

$$\dot{L}(t) \leq -\mu^*(t, T_{\text{con}}) p_{\text{min}}^* K \left(d^{2\beta} + e_\psi^{2\beta} \right). \quad (25)$$

Subsequently, according to Lemma 6, we zoom in on the right half of inequality (25).

$$\left[(d^2)^\beta + (e_\psi^2)^\beta \right] \geq (d^2 + e_\psi^2)^\beta \geq 0, \quad (26)$$

where $1/2 < \beta < 1$. Therefore, inequality (26) can be scaled up to

$$\dot{L}(t) \leq -\mu^*(t, T_{\text{con}}) p_{\text{min}}^* K \left(d^2 + e_\psi^2 \right)^\beta = -2^\beta K p_{\text{min}}^* \mu^*(t, T_{\text{con}}) L^\beta, \quad (27)$$

which is definitely negative since, by definition, $\mu^*(t, T_{\text{con}}) > 0$. Then, inequality (27) can be specifically described as

$$\dot{L}(t) \leq \begin{cases} -2^\beta K p_{\text{min}}^* \frac{1}{T_{\text{con}} - t} L^\beta, & 0 \leq t \leq t_v, \\ -2^\beta K p_{\text{min}}^* \frac{1}{T_{\text{con}} - t_v} L^\beta, & t > t_v. \end{cases} \quad (28)$$

TABLE 1: The model parameters of the DWR.

Symbol	Parameters meaning	Selection advice
k	For adjusting the orientation error (6)	$0 \leq k \leq \frac{1}{2\pi}$
K_e	For adjusting the constraint function (10)	1
K_1, K_2	Controller parameters	$K_1, K_2 > 0$
β, K	For adjusting the time-varying scale function (17)	$\frac{1}{2} < \beta < 1, K = \min \{0.6K_1, K_2\}$
T_{con}	Prescribed-time parameter	$T_{\text{con}} > \frac{d_0}{u_{\text{max}}}$

We solve the differential inequality (27) for the case when time $t \in [0, t_v]$.

$$\int_0^t \frac{1}{L^\beta} dL \leq -2^\beta K p_{\min}^* \int_0^t \frac{1}{T_{\text{con}} - s} ds,$$

$$\frac{1}{1-\beta} L^{1-\beta}(t) \leq \frac{1}{1-\beta} L^{1-\beta}(0) + 2^\beta K p_{\min}^* \ln \left(\frac{T_{\text{con}} - t}{T_{\text{con}}} \right), \quad (29)$$

then,

$$L^{1-\beta}(t) \leq L^{1-\beta}(0) + (1-\beta) 2^\beta K p_{\min}^* \ln \left(\frac{T_{\text{con}} - t}{T_{\text{con}}} \right). \quad (30)$$

From inequality (27), the Lyapunov function L is monotonically decreasing, which implies that the function $L^{1-\beta}$ is also monotonically decreasing. Therefore, when $t \rightarrow \infty$, there must exist some time t_l such that $L^{1-\beta}(t_l) \rightarrow 0$. We can get

$$L^{1-\beta}(0) = -(1-\beta) 2^\beta K p_{\min}^* \ln \left(\frac{T_{\text{con}} - t_l}{T_{\text{con}}} \right), \quad (31)$$

and further obtain an expression for t_l :

$$t_l = T_{\text{con}} \left\{ 1 - \exp \left[-\frac{L^{1-\beta}(0)}{(1-\beta) 2^\beta K p_{\min}^*} \right] \right\}. \quad (32)$$

From equation (17), $t_l = t_v$. Therefore, for the Lyapunov function (21), there is $\lim_{t \rightarrow t_v} L = 0$. This means that when $t \rightarrow t_v$, there is $d, e_\psi \rightarrow 0$, i.e., $\lim_{t \rightarrow t_v} (d, e_\psi) = 0$. Then, when $t > t_w$, we have $d, e_\psi = 0$.

In summary, the control laws (16) and (18) allow the control system (8) of the DWR to be asymptotically stabilized for a set time t_v . This time t_v is prespecified by the prescribed-time parameter T_{con} . The proof is completed. \square

Theorem 7 proves that the system position error converges to 0 within the preset time, which means that the method in this paper achieves the preset time positioning control. Then, robots sometimes need to perform angle con-

trol. Therefore, this paper further proves that after the system is stable, the angle can also be stabilized.

Theorem 8. For the state variable ψ (yaw angle) in system (1), it is prescribed-time stable under the action of the control laws (16) and (18).

Proof. Choose the following auxiliary function $L_\alpha = \alpha^2/2$. Taking its time derivative, we get

$$\dot{L}_\alpha = \alpha \frac{u \sin(e_\psi - \zeta)}{d} = \alpha K_1 \mu^*(t, T_{\text{con}}) p^* d^{2\beta-1} \frac{\sin(e_\psi - \zeta)}{d}. \quad (33)$$

In Theorem 7, we conclude that $|e_\psi|$ decreases gradually to zero at t_v , and remains stable after time t_v . Therefore, when $t \rightarrow t_v$, there is

$$\dot{L}_\alpha \rightarrow -K_1 \mu^*(t, T_{\text{con}}) p^* k d^{2\beta-1} \alpha^2, \quad (34)$$

where \dot{L}_α satisfies $\dot{L}_\alpha \leq 0$ in some neighborhood of time t_v . Second, as $t \rightarrow t_v$, the function L_α will appear monotonically decreasing at this time such that $L_\alpha \rightarrow 0$, i.e., $\lim_{t \rightarrow t_v} \alpha$

$\rightarrow 0$ and $\lim_{t \rightarrow t_v} \zeta \rightarrow 0$. Subsequently, e_ψ is defined as $e_\psi = \alpha - \psi + \zeta$ and satisfies $\lim_{t \rightarrow t_v} e_\psi \rightarrow 0$. Then, we can obtain $\lim_{t \rightarrow t_v} \psi \rightarrow 0$. The proof is completed. \square

Remark 9. Due to the infinite gain risk, conventional PTC methods cannot be directly applied to DWR control systems that require continuous operation [16, 17]. In this paper, a novel time-varying scaling function (17) is designed and used to propose the prescribed-time fractional order position control laws (16) and (18). The proposed controller ensures that the kinematic system of the DWR (8) is prescribed-time globally asymptotically stable in t_v . Then, t_v is predetermined by a prescribed-time parameter T_{con} . This issue ensures that the settling time for the closed-loop system stability is earlier than that of conventional preset time control methods.

The proposed velocity control laws (16) and (18) have the following advantages: (1) Compared with [9], the

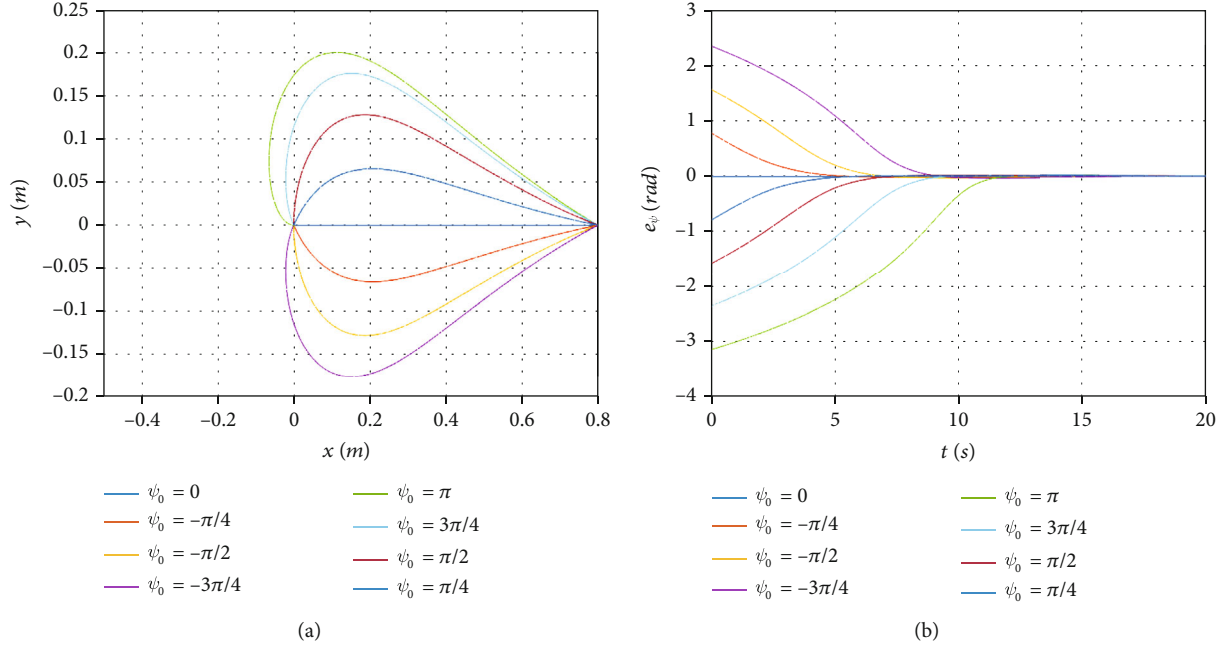


FIGURE 5: Any initial yaw angles. (a) Motion trajectory (b) Orientation error variation.

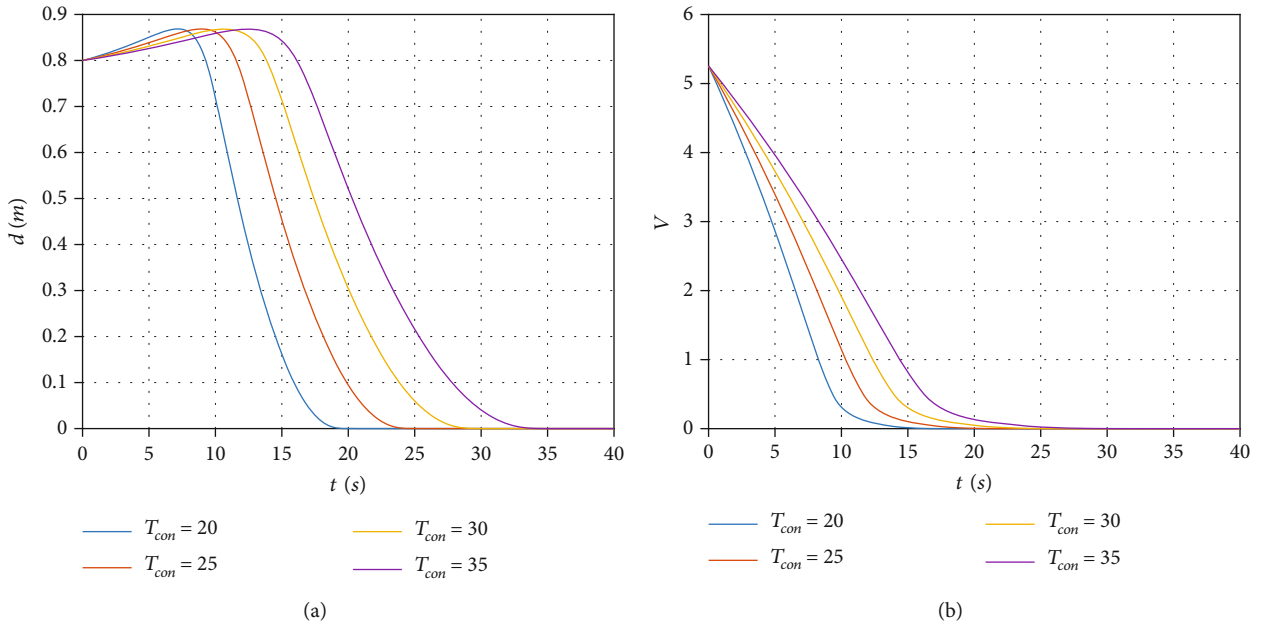


FIGURE 6: Different prescribed-time parameters. (a) Distance (b) Lyapunov function (21).

improved orientation error (6) allows the DWR to reach the target position with its yaw angle remaining at zero. Moreover, the novel orientation error auxiliary function (10) solves the problem that the robot cannot accelerate when the robot yaw angle is opposite to the azimuth angle ($|\alpha - \psi| = \pm\pi$). (2) In contrast to [20], the time-varying scaling function (17) ensures that the DWR's control system is prescribed-time globally asymptotically stable at time t_v , rather than a neighborhood around time t_v .

4.2. Parameter Choosing. The prescribed-time parameter T_{con} is satisfying $0 < d_0/u_{max} < T_{con}$ (u_{max} is the maximum line speed allowed for the robot) and is irrelevant to initial system conditions. $K_0 = 0.1$ is given in literature [9]. Table 1 gives the selection range of controller parameters. To adjust the orientation error, we choose a small parameter k . This is because a large k may cause the robot to rotate too fast and lose accuracy. In the range of less than 1, the smaller parameter β theoretically is, the faster the system stabilizes.

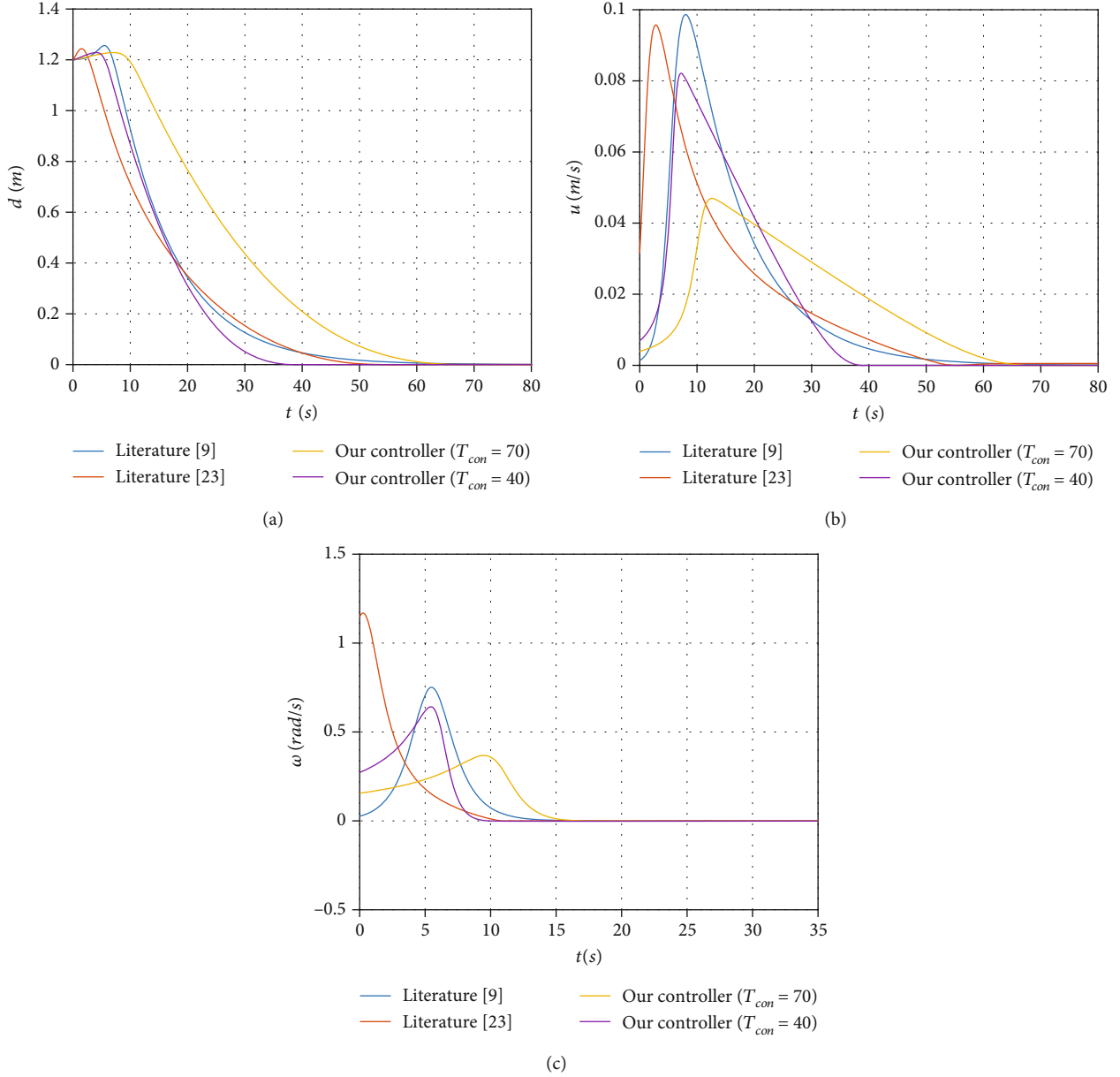


FIGURE 7: Control performance comparison. (a) Distance changes (b) Linear velocity (c) Angular velocity.

But at the same time, it will also cause the smoothness of the control law to deteriorate, which will actually affect performance. Therefore, this paper suggests that the selection of beta should be as large as possible, with a range of $1/2 < \beta < 1$. According to the above statement, the time-varying scale function parameters need to satisfy $K = \min \{0.6K_1, K_2\}$. On the basis of meeting the algorithm requirements, the parameter T_{con} can be selected according to the actual situation. Therefore, the selection of parameters is summarized in this paper as follows.

5. Numerical Simulation

In this section, we used MATLAB to simulate the method mentioned and discussed the results. We first verified the effectiveness of the proposed controller. Subsequently, we

compared the approach of this paper with literatures [9, 23], respectively. First, the effectiveness of control laws (16) and (18) is verified in the numerical simulation in Figures 5 and 6.

The initial position of the selected robot is $(0, 0)$, and the target position is $(0.8, 0)$. The remaining controller parameters are as follows: $K_1 = 2, K_2 = 10, K = 1.2, K_e = 1, T_{con} = 20, \beta = 24/25, k = 1/(2\pi)$. Testing a number of representative initial yaw angles ($\psi_0 = 0, -\pi/4, -\pi/2, -3\pi/4, \pi, 3\pi/4, \pi/2, \pi/4$), Figure 5(a) shows the changes in the coordinates of the robot during position control, and Figure 5(b) shows the changes in the orientation error of the robot during position control. The simulation results show that under any initial yaw angle, the proposed control laws (16) and (18) can enable the robot to reach the endpoint in a prescribed-time T_{con} . When $|\alpha - \psi| = \pi$ ($p = 0$), the

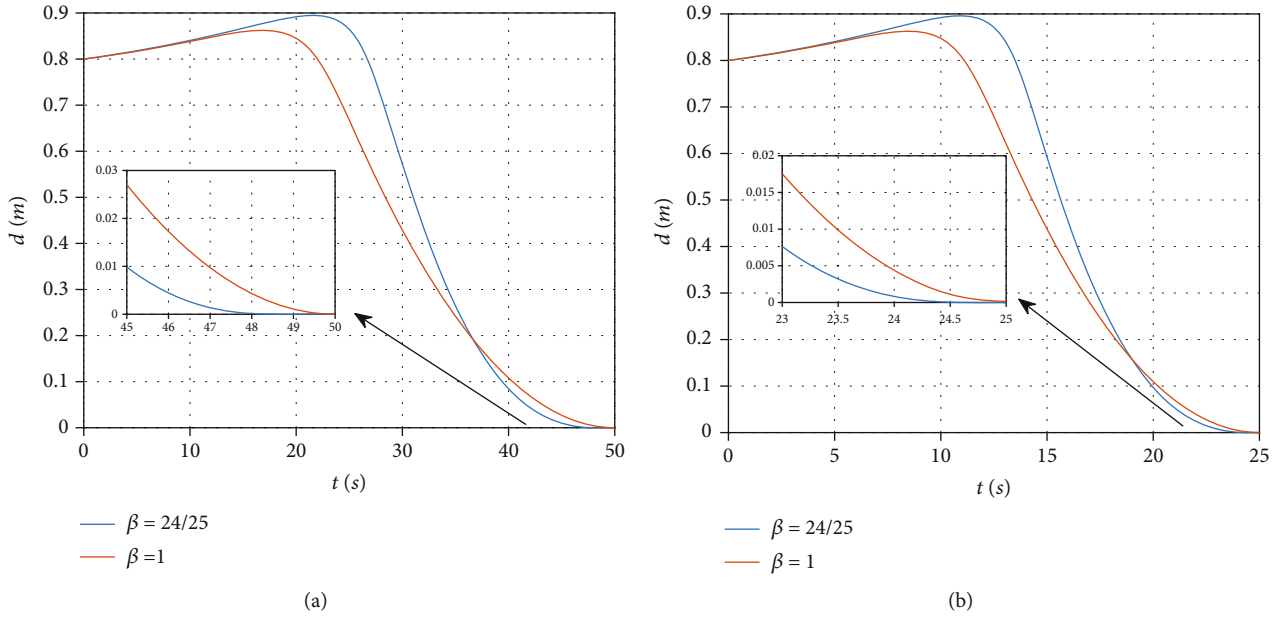
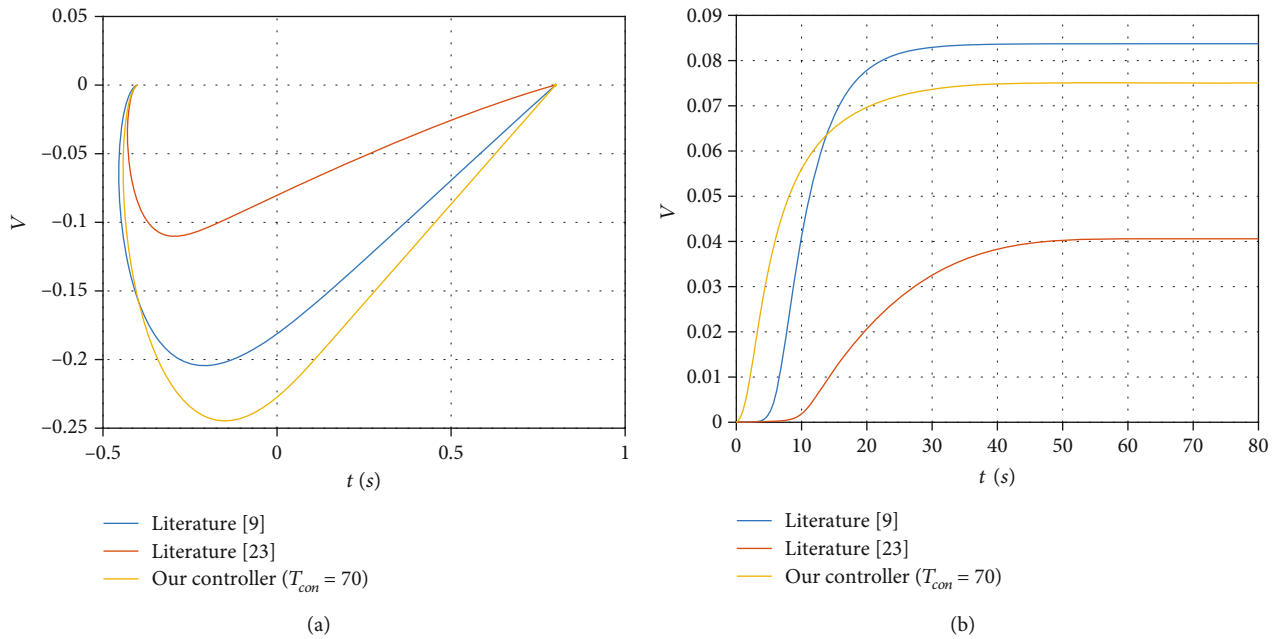
FIGURE 8: Settling time comparison. (a) $T_{con} = 25$. (b) $T_{con} = 50$.

FIGURE 9: Trajectory and energy consumption. (a) Coordinate changes (b) Energy loss.

line velocity in literature [9] is zero, causing error balance points, which may cause the robot not to move correctly. The linear velocity constraint function $p^* > 0$ proposed in this paper avoids this risk.

Subsequently, in Figure 6, set the initial value of the robot's yaw angle to $\psi_0 = \pi$. Figures 6(a) and 6(b) show the effects of different prescribed-time parameters ($T_{con} = 20, 25, 30,$ and 35) on the distance d and the Lyapunov function (21), respectively. The simulation results show that the designed position control law can control the time of robot

arrival at the target position by adjusting T_{con} , and the choice of T_{con} is independent of other design parameters.

Finally, under the same driving conditions, we compare the asymptotically stable control laws in [9], the fixed-time control law in [23], and the control law of this paper. The initial position is fixed to $(-0.4, 0)$, the initial yaw angle $\psi_0 = -178^\circ$, and the target position is $(0.8, 0)$. In literature [9], the control system of the robot reaches a steady state at around $t = 70$ s. Therefore, we set the prescribed-time parameter $T_{con} = 70$ as a way to compare the advantages

and disadvantages of the control strategies. Other parameters are as follows: $K_0 = 0.1$, $K_1 = 2.5$, $K_2 = 40$, $K = 1.2$, $K_e = 1$, $\beta = 24/25$, and $k = 1/(2\pi)$.

Figure 7(a) shows the variation in the distance between the robot and the target position. Although the controller in this paper has no significant advantage in the control effect of distance d , the controller proposed in this paper can adjust the time for the robot to reach the target position by setting the prescribed-time parameter T_{con} , which is not available in other control methods. Figure 7(b) shows the comparison of linear velocity. The results show that the peak linear velocity under the control method of this paper is the lowest for similar settling times. Moreover, Figure 7(c) shows the comparison result of the angular velocity. Due to the fixed time control law of literature [23], there is a high power item with hidden dangers of high control gain, which makes its initial angle speed value significantly higher than other curves. In contrast, this paper's angular velocity control law does not have a high power term and can achieve system convergence within a prescribed time.

To illustrate the role of fractional order control, this paper presents a comparison between control laws with fractional powers and conventional prescribed-time controls. Figures 8(a) and 8(b) respectively show the cases where the prescribed settling times $T_{\text{con}} = 25$ and 50. In order to improve the smoothness of the control law, this paper chooses the fractional power parameter $\beta = 24/25$. The two figures illustrate that compared to the conventional prescribed settling time method, this method can ensure system convergence by using fractional powers before the preset deadline T_{con} , thereby avoiding the risk of the term $1/(T_{\text{con}} - t)$ being infinite at the prescribed settling time.

As shown in Figures 9(a) and 9(b), as regards the robot's arrival at the target position, the control law proposed in this paper has the best trajectory and lower energy consumption.

6. Conclusion

This paper proposes a novel prescribed-time fractional order position controller for the DWR kinematic model. This controller is equipped with a new piecewise time-varying scaling function, which avoids the infinite gain risk faced near the settling time in conventional PTC. Using this controller, the system state of DWR can converge to a bounded interval in a prescribed time, and the prescribed time can be arbitrarily specified within the allowable physical range. Compared with reference [9], the designed linear velocity control law avoids the risk of incorrect balance points. In addition, when implementing position control, the proposed controller has a better movement trajectory and less energy consumption.

Using active disturbance rejection control to compensate for unknown disturbances to the robot is a good solution [24]. Also, when the robot has an actuator failure, DWR's prescribed-time position control will be more complex [18]. In addition, considering combining adaptive control and prescribed-time control is also a topic worth researching [25, 26].

Data Availability

The data is available from the corresponding author upon request. This paper uses MATLAB Simulink for simulation verification.

Conflicts of Interest

The authors declare that the research was conducted in the absence of any commercial or financial relationships that could be construed as a potential conflict of interest.

Acknowledgments

This work was supported by the Natural Science Foundation of Huzhou under grant 2022YZ31, the Huzhou Key Laboratory of Intelligent Sensing and Optimal Control for Industrial Systems under grant 2022-17, the Postgraduate Research and Innovation Project of Huzhou University under grant 2022KYCX58, the Zhejiang Province New Young Talent Plan Project in 2022 under grant 2022R431B021, and the Scientific Research Fund of Zhejiang Provincial Department of Education under the Grant Y202250212.

References

- [1] Y. Chung, C. Park, and F. Harashima, "A position control differential drive wheeled mobile robot," *IEEE Transactions on Industrial Electronics*, vol. 48, no. 4, pp. 853–863, 2001.
- [2] K. Shojaei, A. M. Shahri, A. Tarakameh, and B. Tabibian, "Adaptive trajectory tracking control of a differential drive wheeled mobile robot," *Vehicleica*, vol. 29, no. 3, pp. 391–402, 2011.
- [3] H. Gariblu and M. H. Korayem, "Trajectory optimization of flexible mobile manipulators," *Vehicleica*, vol. 24, no. 3, pp. 333–335, 2006.
- [4] H. Gariblu, A. Heidari, and A. Nikoobin, "Maximum allowable dynamic load of flexible mobile manipulators using finite element approach," *International Journal of Advanced Manufacturing Technology*, vol. 36, no. 9–10, pp. 1010–1021, 2008.
- [5] M. H. Korayem, A. Nikoobin, and V. Azimi, "Maximum load carrying capacity of mobile manipulators: optimal control approach," *Vehicleica*, vol. 27, no. 1, pp. 147–159, 2009.
- [6] M. H. Korayem, V. Azimi, and A. H. Vatanjou, "Maximum load determination of nonholonomic mobile manipulator using hierarchical optimal control," *Vehicleica*, vol. 30, no. 1, pp. 53–65, 2012.
- [7] X. Yu and L. Liu, "Distributed formation control of nonholonomic vehicles subject to velocity constraints," *IEEE Transactions on Industrial Electronics*, vol. 63, no. 2, pp. 1289–1298, 2016.
- [8] S. K. Malu and J. Majumdar, "Kinematics, Localization and Control of Differential Drive Mobile Vehicle," *Global Journal of Research in Engineering*, vol. 14, no. 1, pp. 1–9, 2014.
- [9] E. Fabregas, G. Farias, E. Aranda-Escolastico et al., "Simulation and experimental results of a new control strategy for point stabilization of nonholonomic mobile robots," *IEEE Transactions on Industrial Electronics*, vol. 67, no. 8, pp. 6679–6687, 2020.

- [10] E. Fabregas, G. Farias, S. Dormido-Canto, M. Guinaldo, J. Sánchez, and S. Dormido Bencomo, "Platform for teaching mobile robotics," *Journal of Intelligent & Robotic Systems*, vol. 81, pp. 131–143, 2016.
- [11] F. Pourboghraat and M. P. Karlsson, "Adaptive control of dynamic mobile robots with nonholonomic constraints," *Computers & Electrical Engineering*, vol. 28, no. 4, pp. 241–253, 2002.
- [12] F. Kuhne, W. F. Lages, and J. Silva, "Point stabilization of mobile vehicles with nonlinear model predictive control," in *IEEE International Conference Mechatronics and Automation, 2005*, pp. 1163–1168, Niagara Falls, ON, Canada, 2005.
- [13] P. Zhang, T. Yang, and D. Li, "Formation control of multiple underactuated surface vehicles based on prescribed-time method," *IEEE Access*, vol. 8, pp. 151371–151382, 2020.
- [14] A. Polyakov, D. Efimov, and W. Perruquetti, "Finite-time and fixed-time stabilization: implicit Lyapunov function approach," *Automatica*, vol. 51, pp. 332–340, 2015.
- [15] A. Polyakov, "Nonlinear feedback design for fixed-time stabilization of linear control systems," *IEEE Transactions on Automatic Control*, vol. 57, no. 8, pp. 2106–2110, 2012.
- [16] Y. Song, Y. Wang, J. Holloway, and M. Krstic, "Time-varying feedback for regulation of normal-form nonlinear systems in prescribed finite time," *Automatica*, vol. 83, pp. 243–251, 2017.
- [17] Y. Song, Y. Wang, and M. Krstic, "Time-varying feedback for stabilization in prescribed finite time," *International Journal of Robust Nonlinear Control*, vol. 29, no. 3, pp. 618–633, 2019.
- [18] Z. Wang, B. Liang, Y. Sun, and T. Zhang, "Adaptive fault-tolerant prescribed-time control for teleoperation systems with position error constraints," *IEEE Transactions on Industrial Informatics*, vol. 16, no. 7, pp. 4889–4899, 2020.
- [19] Y. Orlov, R. Kairuz, and L. T. Aguilar, "Prescribed-time robust differentiator design using finite varying gains," *IEEE Control Systems Letters*, vol. 6, pp. 620–625, 2022.
- [20] T. Yang, Y. Ma, P. Zhang, and J. Xu, "Prescribed finite time stabilization of linear systems with state constraints," *IEEE Access*, vol. 9, pp. 47677–47686, 2021.
- [21] A. Shakouri and N. Assadian, "Prescribed-time control with linear decay for nonlinear systems," *IEEE Control Systems Letters*, vol. 6, pp. 313–318, 2022.
- [22] Z. Zuo and L. Tie, "A new class of finite-time nonlinear consensus protocols for multi-agent systems," *International Journal of Control*, vol. 87, no. 2, pp. 363–370, 2014.
- [23] P. Guo, Z. Liang, X. Wang, and M. Zheng, "Adaptive trajectory tracking of wheeled mobile robot based on fixed-time convergence with uncalibrated camera parameters," *ISA Transactions*, vol. 99, pp. 1–8, 2020.
- [24] Y. Wu, L. Wang, J. Zhang, and F. Li, "Path following control of autonomous ground vehicle based on nonsingular terminal sliding mode and active disturbance rejection control," *IEEE Transactions on Vehicular Technology*, vol. 68, no. 7, pp. 6379–6390, 2019.
- [25] X. Huang, Z. Li, C. Wen, and R. He, "Asymptotic parking of general two-trailer systems leveraging singularity," *IEEE Transactions on Industrial Electronics*, vol. 67, no. 9, pp. 7798–7807, 2020.
- [26] P. Krishnamurthy, F. Khorrami, and M. Krstic, "Adaptive output-feedback stabilization in prescribed-time for nonlinear systems with unknown parameters coupled with unmeasured states," *International Journal of Adaptive Control and Signal Processing*, vol. 35, no. 2, pp. 184–202, 2021.